Control of Two-wheeled Mobile Robots Moving in Formation [⋆]

Krzysztof Kozłowski [*] **Wojciech Kowalczyk** [**]

[*] *Poznań University of Technology, Piotrowo 3A, 60-965 Poznań (e-mail: krzysztof.kozlowski@put.poznan.pl)*
[**] *Poznań University of Technology, Piotrowo 3A, 60-965 Poznań (e-mail: wojciech.kowalczyk@put.poznan.pl).*

Abstract: This paper presents control algorithm for multiple non-holonomic mobile robots moving in formation. Method from Canudas et al. (1994) is used to track desired trajectory. In the new algorithm this approach is combined with collision avoidance. Artificial potential functions are used to generate repulsive component of the control. Stability analysis is based on Lyapunov-like function. Effectiveness of the presented method is illustrated by simulation results for a large formation of mobile platforms. Robots avoid collisions with each other and with static obstacles. Position and orientation reach values close to steady state in $50s$.

Keywords: robot formation, non-holonomic robot, trajectory tracking, stability analysis, Lyapunov-like function

1. INTRODUCTION

In 1980s Khatib (1986) proposed to use artificial potential fields in the control of manipulators and mobile robots. In this approach both attraction to the goal and repulsion from the obstacles are negated gradient of the *Artificial Potential Function* (APF). Khatib (1986) presented in-depth theoretical analysis and illustrated it by the practical application. Much earlier, in 1977 Leitmann and Skowronski (1977) investigated control of two agents avoiding collisions with each other. Their work was, however, purely theoretical.

Since 1990s the problem of trajectory tracking control for differentially-driven mobile robots was widely investigated: Canudas et al. (1994), Morin and Samson (2003), Kowalczyk et al. (2012). Recently, number of articles in subject of the control for robot formations have been published: Do (2008), Mastellone et al. (2008), Kowalczyk et al. (2010), Kowalczyk and Kozłowski (2018). In Yoo and Park (2019) an alternative approach is presented in which APFs are not used. Nonlinear formation error based on relative distances and angles between robots are used to preserve connectivity and collision avoidance.

Contribution of this paper is to propose a new control algorithm that efficiently converges for a large formation of robots. It is based on the trajectory tracking algorithm proposed by Canudas et al. (1994). Collision avoidance was included in the new control algorithm and is guaranteed. The obstacles are assumed to be circular shaped. Robots avoid collisions with each other and with static obstacles existing in the environment. Lyapunov-like function approach is used in stability analysis. Tracking errors are reduced to small values. The convergence for a complex case is confirmed by numerical simulation.

In Section 2 model of the system is introduced. Task of the multi-robot formation is described in Section 3. Section 4 introduces APFs used to avoid collisions between robots and with obstacles. In Section 5 control algorithm for the group of differentially-driven mobile robots is presented. In Section 6 stability analysis is given. Simulation results are presented in Section 7. In the last section concluding remarks are given.

2. MODEL OF THE SYSTEM

The kinematic model of the i-th two-wheeled mobile robot R_i ($i = 1 \dots N$, N - number of robots) is given by the following equation:

$$\dot{q}_i = \begin{bmatrix} \cos\theta_i & 0 \\ \sin\theta_i & 0 \\ 0 & 1 \end{bmatrix} u_i \tag{1}$$

where vector $q_i = [x_i \;\; y_i \;\; \theta_i]^\top$ denotes the pose and x_i, y_i, θ_i are position coordinates and orientation of the robot with respect to a global, fixed coordinate frame. Vector $u_i = [v_i \; \omega_i]^\top$ is the control vector with v_i denoting linear velocity control and ω_i denoting angular velocity control of the platform.

3. THE TASK

The task of the formation is to follow virtual leader that moves with desired linear and angular velocities $[v_l \;\; \omega_l]^T$ along planed trajectory. The robots are expected to imitate the motion of the virtual leader. They should have the same velocities as the virtual leader. The position coordinates $[x_l \;\; y_l]^T$ of the virtual leader are used as a reference position of the individual robots but each of them have different spatial displacement with respect to the leader:

[⋆] This work is supported by statutory grant 09/93/DSPB/0811.

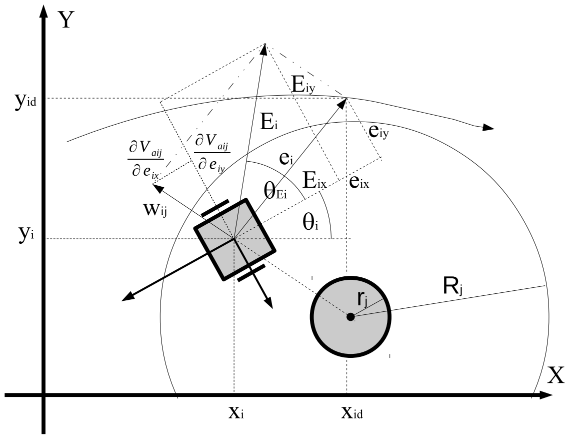

Fig. 1. Robot in the environment with obstacle

$$
\begin{aligned}
x_{id} &= x_l + d_{ix}\\
y_{id} &= y_l + d_{iy},
\end{aligned}
\tag{2}
$$

where $[d_{ix} \quad d_{iy}]^T$ is a desired displacement of the i-th robot. As the robots position converge to the desired values their orientations θ_i converge to the orientation of the virtual leader θ_l.

4. ARTIFICIAL POTENTIAL FUNCTION

Collision avoidance behaviour is based on the APF. All robots are surrounded by APFs that raise to infinity near objects border r_j (j - number of the robot/obstacle) and decreases to zero at some distance R_j, $R_j > r_j$.

One can introduce the following function Kowalczyk et al. (2012):

$$
B_{aij}(l_{ij}) = \begin{cases} 0 & \text{for} \quad l_{ij} < r_j \\ e^{\frac{l_{ij}-r_j}{l_{ij}-R_j}} & \text{for } r_j \leq l_{ij} < R_j \\ 0 & \text{for} \quad l_{ij} \geq R_j \end{cases}, \tag{3}
$$

that gives output $B_{aij}(l_{ij}) \in \langle 0, 1)$. Distance between the i-th robot and the j-th obstacle (or robot) is defined as the Euclidean length $l_{ij} = \left\| [x_j \; y_j]^\top - [x_i \; y_i]^\top \right\|$.

Scaling the function given by Eq. (3) within the range $\langle 0, \infty)$ can be given as follows:

$$
V_{aij}(l_{ij}) = \frac{B_{aij}(l_{ij})}{1 - B_{aij}(l_{ij})}, \tag{4}
$$

that is used later to avoid collisions.

In further description terms 'collision area' or 'collision region' is used for locations fulfilling conditions $l_{ij} < r_j$. The range $r_j < l_{ij} < R_j$ is called 'collision avoidance area' or 'collision avoidance region'.

5. CONTROL ALGORITHM

The goal of the control is to drive the formation along the desired trajectory avoiding collisions between agents. It is equivalent to bringing the following quantities to zero:

$$
\begin{aligned}
p_{ix} &= x_{id} - x_i\\
p_{iy} &= y_{id} - y_i\\
p_{i\theta} &= \theta_l - \theta_i.
\end{aligned}
\tag{5}
$$

Assumption 1. $\forall \{i, j\}, i \neq j,\ ||[x_{id} \;\; y_{id}]^T - [x_{jd} \;\; y_{jd}]^T|| > R_j$.

Assumption 2. If robot i gets into avoidance region with any other robot j, $j \neq i$ its desired trajectory is temporarily frozen ($\dot{x}_{id} = 0$, $\dot{y}_{id} = 0$). If the robot leaves the avoidance area its desired coordinates are immediately updated. As long as the robot remains in the avoidance region its desired coordinates are periodically updated at certain discrete instants of time. The time period t_u of this update process is relatively large in comparison to the main control loop sample time.

Assumption 1 comes down to the statement that desired paths of individual robots are planned in such a way that in the steady state all robots are outside of the collision avoidance regions of other robots.

Assumption 2 means that tracking process is temporarily suspended because collision avoidance has a higher priority. Once the robot is outside the collision detection region, it updates the reference to the new values. In addition when the robot is in the collision avoidance region its reference trajectory is periodically updated. It supports leaving the unstable equilibrium points (that occurs, e.g. when one robot is located exactly between the other robots and its goal) if the reference trajectory is exciting enough. In rare cases, the robot may get stuck at a saddle point, but the set of such points is of measure zero and will not be considered further.

The system error expressed with respect to the coordinate frame fixed to the robot is described below:

$$
\begin{bmatrix} e_{ix} \\ e_{iy} \\ e_{i\theta} \end{bmatrix} = \begin{bmatrix} \cos(\theta_i) & \sin(\theta_i) & 0 \\ -\sin(\theta_i) & \cos(\theta_i) & 0 \\ 0 & 0 & 1 \end{bmatrix} \begin{bmatrix} p_{ix} \\ p_{iy} \\ p_{i\theta} \end{bmatrix}. \tag{6}
$$

Using the above equations and non-holonomic constraint $\dot{y}_i \cos(\theta_i) - \dot{x}_i \sin(\theta_i) = 0$ the error dynamics are as follows:

$$
\begin{aligned}
\dot{e}_{ix} &= e_{iy}\omega_i - v_i + v_l \cos e_{i\theta}\\
\dot{e}_{iy} &= -e_{ix}\omega_i + v_l \sin e_{i\theta}\\
\dot{e}_{i\theta} &= \omega_l - \omega_i,
\end{aligned}
\tag{7}
$$

where v_l and ω_l are controls of the reference (virtual) vehicle followed by the formation. One can introduce the position correction variables that consist of position error and collision avoidance terms:

$$
\begin{aligned}
P_{ix} &= p_{ix} - \sum_{j=1, j\neq i}^{N+M} \frac{\partial V_{aij}}{\partial x_i}\\
P_{iy} &= p_{iy} - \sum_{j=1, j\neq i}^{N+M} \frac{\partial V_{aij}}{\partial y_i}.
\end{aligned}
\tag{8}
$$

V_{aij} depends on x_i and y_i according to equation (4); M is a number of static obstacles. Robots avoid collisions with static obstacles and with each other. The correction variables can be transformed to the local coordinate frame fixed to the geometric centre of the robot:

$$
\begin{bmatrix} E_{ix} \\ E_{iy} \\ e_{i\theta} \end{bmatrix} = \begin{bmatrix} \cos(\theta_i) & \sin(\theta_i) & 0 \\ -\sin(\theta_i) & \cos(\theta_i) & 0 \\ 0 & 0 & 1 \end{bmatrix} \begin{bmatrix} P_{ix} \\ P_{iy} \\ p_{i\theta} \end{bmatrix}. \tag{9}
$$

Differentiating first two equations of (5) with respect to the p_{ix} and p_{iy} respectively one obtains:

$$\begin{aligned}\frac{\partial x_i}{\partial p_{ix}} &= -1\\ \frac{\partial y_i}{\partial p_{iy}} &= -1.\end{aligned}\tag{10}$$

Using (10) one can write:

$$\begin{aligned}\frac{\partial V_{aij}}{\partial p_{ix}} &= \frac{\partial V_{aij}}{\partial x_i}\frac{\partial x_i}{\partial p_{ix}} = -\frac{\partial V_{aij}}{\partial x_i}\\ \frac{\partial V_{aij}}{\partial p_{iy}} &= \frac{\partial V_{aij}}{\partial y_i}\frac{\partial y_i}{\partial p_{iy}} = -\frac{\partial V_{aij}}{\partial y_i}.\end{aligned}\tag{11}$$

Now gradient of the APF can be expressed with respect to the local coordinate frame fixed to the i-th robot and is calculated as follows:

$$\begin{bmatrix}\dfrac{\partial V_{aij}}{\partial e_{ix}}\\ \dfrac{\partial V_{aij}}{\partial e_{iy}}\end{bmatrix} = \begin{bmatrix}\cos\theta_i & \sin\theta_i\\ -\sin\theta_i & \cos\theta_i\end{bmatrix}\begin{bmatrix}\dfrac{\partial V_{aij}}{\partial p_{ix}}\\ \dfrac{\partial V_{aij}}{\partial p_{iy}}\end{bmatrix}.\tag{12}$$

Equation (12) can be verified easily by taking partial derivatives of $V_{aij}(d_{ix} - p_{ix}, d_{iy} - p_{iy}) = V_{aij}(d_{ix} - p_{ix}(e_{ix}, e_{iy}), d_{iy} - p_{iy}(e_{ix}, e_{iy}))$ with respect to e_{ix}, e_{iy} and taking into account inverse transformation of the first two equations of (6).

Using (11) above equation can be written as follows:

$$\begin{bmatrix}\dfrac{\partial V_{aij}}{\partial e_{ix}}\\ \dfrac{\partial V_{aij}}{\partial e_{iy}}\end{bmatrix} = \begin{bmatrix}-\cos\theta_i & -\sin\theta_i\\ \sin\theta_i & -\cos\theta_i\end{bmatrix}\begin{bmatrix}\dfrac{\partial V_{aij}}{\partial x_i}\\ \dfrac{\partial V_{aij}}{\partial y_i}\end{bmatrix}.\tag{13}$$

Equations (9) using (8) and (13) can be transformed to the following form:

$$\begin{aligned}E_{ix} &= p_{ix}\cos(\theta_i) + p_{iy}\sin(\theta_i) + \sum_{j=1,j\neq i}^{N+M}\frac{\partial V_{aij}}{\partial e_{ix}}\\ E_{iy} &= -p_{ix}\sin(\theta_i) + p_{iy}\cos(\theta_i) + \sum_{j=1,j\neq i}^{N+M}\frac{\partial V_{aij}}{\partial e_{iy}}\\ e_{i\theta} &= p_{i\theta}\end{aligned}\tag{14}$$

where each derivative of the APF is transformed form the global coordinate frame to the local coordinate frame fixed to the robot. Finally, correction variables expressed with respect to the local coordinate frame are as follows:

$$\begin{aligned}E_{ix} &= e_{ix} + \sum_{j=1,j\neq i}^{N+M}\frac{\partial V_{aij}}{\partial e_{ix}}\\ E_{iy} &= e_{iy} + \sum_{j=1,j\neq i}^{N+M}\frac{\partial V_{aij}}{\partial e_{iy}}.\end{aligned}\tag{15}$$

Note the similarity of the structure of equations (8) and (15) when the last one is updated by Eq. (13). In Fig. 1 exemplary situation with a single robot and a single obstacle is presented ($w_{ij} = \left[\frac{\partial V_{aij}}{\partial e_{ix}}\ \frac{\partial V_{aij}}{\partial e_{iy}}\right]^T$).

Trajectory tracking algorithm from Canudas et al. (1994) combined with collision avoidance for N robots and M static obstacles can be written as follows:

$$\begin{aligned}v_i &= v_l\cos e_{i\theta} + k_1 E_{ix}\\ \omega_i &= \omega_l + k_2\mathrm{sgn}(v_l)E_{iy} + k_3 e_{i\theta}\end{aligned}\tag{16}$$

where k_1, k_2, k_3 are constant parameters greater then zero and function sgn($\bullet$) is defined as follows:

$$\mathrm{sgn}(\xi) = \begin{cases}-1 & \text{for } \xi < 0\\ 0 & \text{for } \xi = 0\\ 1 & \text{for } \xi > 0\end{cases}.$$

Regardless of the definition of sgn($\bullet$) function for $v_l = 0$ we propose to keep second term in Eq. (16) as k_2E_{iy} in order to avoid possible deadlock.

Assumption 3. If the value of the linear control signal is less then considered threshold value v_t, i.e. $|v_i| < v_t$ (v_t - positive constant), it is replaced by a new scalar function $\tilde{v}_i = S(v_i)v_t$, where

$$S(v) = \begin{cases}-1 & \text{for } v < 0\\ 1 & \text{for } v \geq 0\end{cases}.\tag{17}$$

Substituting (16) into (7) error dynamics is given by the following equations:

$$\begin{aligned}\dot{e}_{ix} &= e_{iy}\omega_i - k_1E_{ix}\\ \dot{e}_{iy} &= -e_{ix}\omega_i + v_l\sin e_{i\theta}\\ \dot{e}_{i\theta} &= -k_2\mathrm{sgn}(v_l)E_{iy} - k_3e_{i\theta}\end{aligned}\ .\tag{18}$$

Transforming (18) using (16) and taking into account Assumption 2 (when robot gets into collision avoidance region, velocities v_l and ω_l are substituted as 0) error dynamics can be expressed in the following form:

$$\begin{aligned}\dot{e}_{ix} &= k_3e_{iy}e_{i\theta} + k_2e_{iy}E_{iy} - k_1E_{ix}\\ \dot{e}_{iy} &= -k_3e_{ix}e_{i\theta} - k_2e_{ix}E_{iy}\\ \dot{e}_{i\theta} &= -k_2E_{iy} - k_3e_{i\theta}\end{aligned}\ .\tag{19}$$

Regardless to the fact that $v_l = 0$ in the collision avoidance region we propose to keep k_2E_{iy} in Eq. (16).

6. STABILITY OF THE SYSTEM

In this section stability analysis of the closed-loop system is presented. When the i-th robot is not in the collision regions of the other robots (APF takes the value zero) the analysis given in Canudas et al. (1994) is valid and will be no repeated here. Further the analysis for the situation in which the i-th robot is in the collision region of other robot is presented.

For further analysis a new variable is introduced: $\theta_{iE} = Atan2(E_{iy}, E_{ix})$ [1] - auxiliary orientation variable.

Proposition 1. The system (1) with controls (16) is stable if the desired trajectories fulfil the condition $\theta_{iE} \notin \left\langle\frac{\pi}{2} \pm \theta_{E\Delta} \pm \pi d\right\rangle$ ($d = 0, \pm1, \pm2, ...$), where $\theta_{E\Delta}$ is a small constant.

Proof 1. Consider the following Lyapunov-like function:

$$V = \sum_{i=1}^{N}\left[\frac{1}{2}(e_{ix}^2 + e_{iy}^2 + e_{i\theta}^2) + \sum_{j=1,j\neq i}^{N+M}V_{aij}\right].\tag{20}$$

If the robot is in the collision avoidance region of the other robot time derivative of the Lyapunov-like function is calculated as follows:

$$\begin{aligned}\frac{dV}{dt} =& \sum_{i=1}^{N}\Big[e_{ix}\dot{e}_{ix} + e_{iy}\dot{e}_{iy} + e_{i\theta}\dot{e}_{i\theta}\\ &+ \sum_{j=1,j\neq i}^{N+M}\left(\frac{\partial V_{aij}}{\partial e_{ix}}\dot{e}_{ix} + \frac{\partial V_{aij}}{\partial e_{iy}}\dot{e}_{iy}\right)\Big].\end{aligned}\tag{21}$$

[1] $Atan2(\bullet, \bullet)$ is a version of the $Atan(\bullet)$ function covering all four quarters of the Euclidean plane

Taking into account Eqs. (15) the above formula can be transformed to the following form:

$$\frac{dV}{dt} = \sum_{i=1}^{N} \left[E_{ix}\dot{e}_{ix} + E_{iy}\dot{e}_{iy} + e_{i\theta}\dot{e}_{i\theta}\right]. \tag{22}$$

Next, using Eq. (19) one obtains:

$$\begin{aligned}\dot{V} = \sum_{i=1}^{N} \big[&k_3 E_{ix} e_{iy} e_{i\theta} + k_2 E_{ix} e_{iy} E_{iy} - k_1 E_{ix}^2 \\ &-k_3 E_{iy} e_{ix} e_{i\theta} - k_2 e_{ix} E_{iy}^2 - k_2 E_{iy} e_{i\theta} - k_3 e_{i\theta}^2\big].\end{aligned} \tag{23}$$

Substituting $E_{ix} = D_i \cos\theta_{iE}$, $E_{iy} = D_i \sin\theta_{iE}$ and $D_i = \sqrt{E_{ix}^2 + E_{iy}^2}$ in the above equation one obtains:

$$\begin{aligned}\dot{V} = \sum_{i=1}^{N} \big[&k_3 D_i \cos\theta_{iE} e_{iy} e_{i\theta} + k_2 D_i^2 e_{iy} \cos\theta_{iE} \sin\theta_{iE} \\ &- k_1 D_i^2 \cos^2\theta_{iE} - k_3 D_i \sin\theta_{iE} e_{ix} e_{i\theta} \\ &- k_2 e_{ix} D_i^2 \sin^2\theta_{iE} - k_2 e_{i\theta} D_i \sin\theta_{iE} - k_3 e_{i\theta}^2\big].\end{aligned} \tag{24}$$

Using an identity substitution

$$-k_3\,\mathrm{e}_{i\theta}^2 = -\frac{1}{3}k_3\,\mathrm{e}_{i\theta}^2 - \frac{1}{3}k_3\,\mathrm{e}_{i\theta}^2 - \frac{1}{3}k_3\,\mathrm{e}_{i\theta}^2 \tag{25}$$

equation (24) can be rewritten as follows:

$$\begin{aligned}\dot{V} = \sum_{i=1}^{N} \Bigg[&(k_3 D_i \cos\theta_{iE} e_{iy} e_{i\theta} - \frac{1}{3}k_3\,\mathrm{e}_{i\theta}^2) \\ &+ (-k_3 D_i \sin\theta_{iE} e_{ix} e_{i\theta} - \frac{1}{3}k_3\,\mathrm{e}_{i\theta}^2) \\ &+ (-k_2 D_i e_{i\theta} \sin\theta_{iE} - \frac{1}{3}k_3\,\mathrm{e}_{i\theta}^2) \\ &+ k_2 D_i^2 e_{iy} \cos\theta_{iE} \sin\theta_{iE} \\ &- k_1 D_i^2 \cos^2\theta_{iE} - k_2 e_{ix} D_i^2 \sin^2\theta_{iE}\Bigg] \\ = \sum_{i=1}^{N} \Bigg\{ &- \Bigg[k_3 \left(\frac{1}{\sqrt{3}} e_{i\theta} - \frac{\sqrt{3}}{2} D_i \cos\theta_{iE} e_{iy}\right)^2 \\ &- k_3 \frac{3}{4} D_i^2 \cos^2\theta_{iE} e_{iy}^2\Bigg] \\ &- k_3 \Bigg[\left(\frac{1}{\sqrt{3}} e_{i\theta} + D_i \sin\theta_{iE} e_{ix} \frac{\sqrt{3}}{2}\right)^2 \\ &- D_i^2 \frac{3}{4} \sin^2\theta_{iE}\,\mathrm{e}_{ix}^2\Bigg] \\ &- \Bigg[\left(\frac{\sqrt{k_3}}{\sqrt{3}} e_{i\theta} + \frac{\sqrt{3}}{2\sqrt{k_3}} k_2 D_i \sin\theta_{iE}\right)^2 \\ &- \frac{3}{4k_3} k_2^2 D_i^2 \sin^2\theta_{iE}\Bigg] \\ &+ k_2 D_i^2 e_{iy} \cos\theta_{iE} \sin\theta_{iE} \\ &- k_1 D_i^2 \cos^2\theta_{iE} - k_2 e_{ix} D_i^2 \sin^2\theta_{iE}\Bigg\}.\end{aligned}$$

To simplify further calculations new scalar functions are introduced:

$$\begin{aligned} a_i &= \frac{1}{\sqrt{3}} e_{i\theta} - \frac{\sqrt{3}}{2} D_i \cos\theta_{iE} e_{iy}, \\ b_i &= \frac{1}{\sqrt{3}} e_{i\theta} + D_i \sin\theta_{iE} e_{ix} \frac{\sqrt{3}}{2}, \\ c_i &= \frac{\sqrt{k_3}}{\sqrt{3}} e_{i\theta} + \frac{\sqrt{3}}{2\sqrt{k_3}} k_2 D_i \sin\theta_{iE}. \end{aligned} \tag{26}$$

Taking into account (26) $\dot{V}$ can be written as follows:

$$\begin{aligned}\dot{V} = \sum_{i=1}^{N} \Bigg\{&-k_3 a_i^2 + k_3 \frac{3}{4} D_i^2 \cos^2\theta_{iE} e_{iy}^2 \\ &- k_3 b_i^2 + k_3 D_i^2 \frac{3}{4} \sin^2\theta_{iE}\,\mathrm{e}_{ix}^2 \\ &- c_i^2 + \frac{3}{4k_3} k_2^2 D_i^2 \sin^2\theta_{iE} \\ &+ k_2 D_i^2 e_{iy} \cos\theta_{iE} \sin\theta_{iE} \\ &- k_1 D_i^2 \cos^2\theta_{iE} - k_2 e_{ix} D_i^2 \sin^2\theta_{iE}\Bigg\}.\end{aligned}$$

Combining and transforming the second and the seventh terms, and the fourth and the eight terms respectively one can write time derivative of the Lyapunov-like function as follows:

$$\begin{aligned}\dot{V} = \sum_{i=1}^{N} \Bigg\{&D_i^2 \sin^2\theta_{iE} \left(\frac{\sqrt{3k_3}}{2} e_{ix} - \frac{1}{\sqrt{3k_3}} k_2\right)^2 \\ &- D_i^2 \sin^2\theta_{iE} \frac{1}{3k_3} k_2^2 \\ &+ \left(\frac{\sqrt{3k_3}}{2} D_i \cos\theta_{iE} e_{iy} + D_i \sin\theta_{iE} k_2 \frac{1}{\sqrt{3k_3}}\right)^2 \\ &- \frac{1}{3k_3} k_2^2 D_i^2 \sin^2\theta_{iE} - k_3 a_i^2 - k_3 b_i^2 - c_i^2 \\ &+ \frac{3}{4k_3} k_2^2 D_i^2 \sin^2\theta_{iE} - k_1 D_i^2 \cos^2\theta_{iE}\Bigg\}.\end{aligned}$$

In the next step the second, the fourth and the last terms are combined and transformed as follows:

$$\begin{aligned}\dot{V} = \sum_{i=1}^{N} \Bigg\{&D_i^2 \sin^2\theta_{iE} \left(\frac{\sqrt{3k_3}}{2} e_{ix} - \frac{1}{\sqrt{3k_3}} k_2\right)^2 \\ &+ \left(\frac{\sqrt{3k_3}}{2} D_i \cos\theta_{iE} e_{iy} + D_i \sin\theta_{iE} k_2 \frac{1}{\sqrt{3k_3}}\right)^2 \\ &- k_3 a_i^2 - k_3 b_i^2 - c_i^2 + \frac{1}{12k_3} k_2^2 D_i^2 \sin^2\theta_{iE} \\ &- k_1 D_i^2 \cos^2\theta_{iE}\Bigg\}.\end{aligned}$$

The closed-loop system is stable ($\dot{V} \leq 0$) if the following condition is fulfilled:

$$\begin{aligned}\sum_{i=1}^{N} \Bigg[&k_1 D_i^2 \cos^2\theta_{iE} - \frac{1}{12k_3} k_2^2 D_i^2 \sin^2\theta_{iE} \\ &- \left(\frac{\sqrt{3k_3}}{2} D_i \cos\theta_{iE} e_{iy} + D_i \sin\theta_{iE} k_2 \frac{1}{\sqrt{3k_3}}\right)^2 \\ &- D_i^2 \sin^2\theta_{iE} \left(\frac{\sqrt{3k_3}}{2} e_{ix} - \frac{1}{\sqrt{3k_3}} k_2\right)^2\Bigg] \geq 0.\end{aligned} \tag{27}$$

As $\cos^2\theta_{iE} > 0$ due to Assumption 3 ($|v_i| > 0$ in a 'freeze' state, i.e. for $v_i = k_1 E_{ix}$ ensure $E_{ix} \neq 0$ that leads to $\theta_{iE} \neq \pm\frac{\pi}{2} \pm \pi d$ $(d = 0, \pm 1, \pm 2, ...)$), the condition (27) can be met by setting sufficiently high value of k_1.

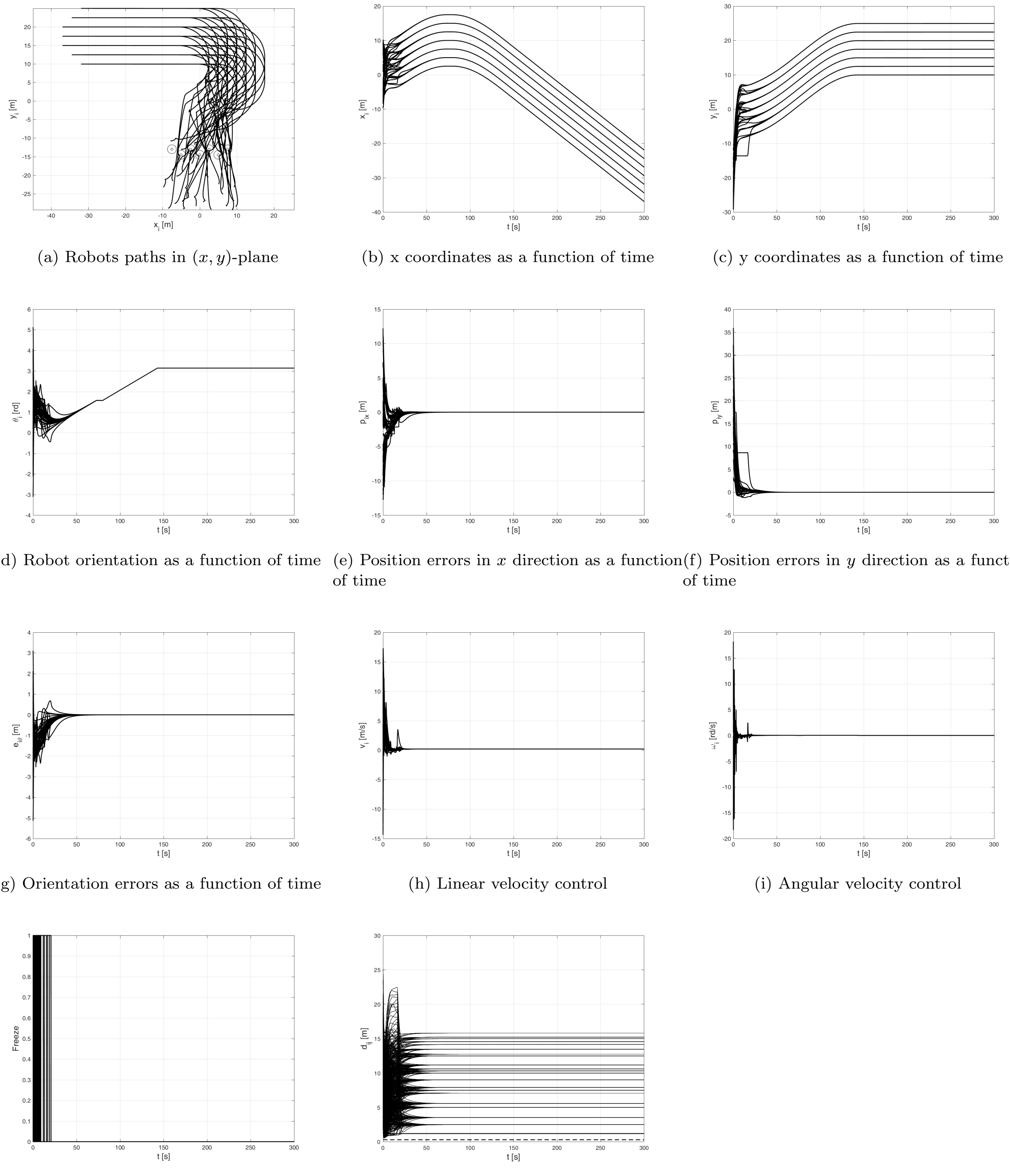

(a) Robots paths in (x, y)-plane

(b) x coordinates as a function of time

(c) y coordinates as a function of time

(d) Robot orientation as a function of time

(e) Position errors in x direction as a function of time

(f) Position errors in y direction as a function of time

(g) Orientation errors as a function of time

(h) Linear velocity control

(i) Angular velocity control

(j) 'Freeze' signal

(k) Distances between robots

Fig. 2. Numerical simulation - trajectory tracking for $N = 37$ robots

As shown in Mastellone et al. (2008) collision avoidance is guaranteed if $\dot{V}_{aij} \leq 0$ and $\lim_{||[x_i\ y_i]^\top - [x_j\ y_j]^\top|| \to r^+} V_{aij} = +\infty$, $i \neq j$.

7. SIMULATION RESULTS

In this section numerical simulation for a group of $N = 37$ mobile robots is presented. Initial coordinates (both positions and orientations) are random. Formation goal is to move along straight lines and arcs. The assignments of robots to particular goal points are random and in the initial state they are located far from the desired trajectory. In addition the area where the desired trajectory passes is separated from the region where most of the robots are located initially with a 'barrier' of static obstacles (Fig. 2a). The passages between these obstacles are narrow.

The following settings of the algorithm are used: $k_1 = 0.5$, $k_2 = 0.5$, $k_3 = 1.0$, $t_u = 1s$, $r = 0.3m$, $R = 1.2m$ (r and R are the same for robots and static obstacles). The value of R_j determines the distance at which the robot begins to react to the presence of an obstacle. In practice, its value should be set taking into account the dynamics of drives and their limitations. The value of t_u can be set to arbitrarily small number, however, it increases the frequency of discontinuities in the control (reference update).

In Fig. 2a paths of robots in the (x, y) plane are shown. Figs. 2b and 2c present graphs of x and y coordinates as a function of time. Robots converge to the desired values with acceptable errors in $50s$. In Fig. 2d time graph of the orientations is shown. In Figs. 2e and 2f components of position errors expressed in global coordinate frame are presented. In Fig. 2g orientation errors are shown. All errors (position and orientation) are reduced to values less then 10^{-13} in $75s$.

In Figs. 2h and 2i linear and angular velocity controls respectively are drawn. Initially and in the transient states their values are high, exceeding maximum values of typical mobile platform. In practical implementation they should be scaled down to realizable values. Fig. 2j presents time graph of the 'freeze' signal (refer to Assumption 2) of robots. Note that the value 1 of the signal represents activity of the collision avoidance block. Although the drawing is not easily readable (because it includes 'freeze' signal of all robots), one can see that the last collision avoidance interaction ends in about $50s$. In Fig. 2k relative distances between robots are shown (notice that the number of signal is $N(N-1) = 1332$). An important information that can be read from this drawing is that no pair of robots reaches inter-agent distance lower or equal to $r = 0.3m$ (dashed line). The smallest inter-agent distance observed during the test was $0.455m$. This minds that no collision occurred between agents.

The authors also verified efficiency of the system for larger formations. The convergence in these cases were obviously slower, due to significantly greater number of interactions between agents, but overall task execution worked well.

8. CONCLUSION

In this paper a new control algorithm for the formation of non-holonomic mobile robots is presented. Robots avoid collision with each other and with static obstacles present is the task space. Lyapunov-like function is used in stability analysis. The algorithm is verified by numerical simulations for a large group of non-holonomic mobile robots moving in formation avoiding collisions with 'barrier' of static, circle shaped obstacles. Author plans to conduct extensive tests of the presented algorithm using real two-wheeled mobile robots in the near future.

REFERENCES

G. Leitmann, J. Skowronski, Avoidance control. J. Optim. Theory Appl. 23(4), pp. 581-591, 1977.

C. Canudas de Wit, H. Khennouf, C. Samson, and O. J. Sordalen, Nonlinear Control Design for Mobile Robots, Recent Trends in Mobile Robots, pp. 121-156, 1994.

P. Morin, C. Samson, Practical stabilization of driftless systems on Lie groups: the transverse function approach, IEEE Transactions on Automatic Control, Vol. 48, Issue 9, pp. 1496-1508, 2003.

O. Khatib, Real-time obstacle avoidance for manipulators and mobile robots, The International Journal of Robotics Research, Vol 5, No. 1, pp. 90-98, 1986.

H. K. Khalil, Nonlinear Systems, 3rd ed. New York, NY, USA, Prentice-Hall, 2002.

S. Mastellone, D. Stipanovic, M. Spong, Formation control and collision avoidance for multi-agent non-holonomic systems: Theory and experiments, The International Journal of Robotics Research, pp. 107-126, 2008.

W. Kowalczyk and M. Michałek and K. Kozłowski, Trajectory tracking control with obstacle avoidance capability for unicycle-like mobile robot, Bulletin of the Polish Academy of Sciences Technical Sciences, Vol. 60, No. 3, pp. 537-546, 2012.

K. D. Do, Formation tracking control of unicycle-type mobile robots with limited sensing ranges, in IEEE Transactions on Control Systems Technology, vol. 16, no. 3, pp. 527-538, May 2008, DOI: 10.1109/TCST.2007.908214

W. Kowalczyk, K. Kozłowski and J. K. Tar, Trajectory tracking for multiple unicycles in the environment with obstacles, 19th International Workshop on Robotics in Alpe-Adria-Danube Region (RAAD 2010), Budapest, 2010, pp. 451-456, DOI: 10.1109/RAAD.2010.5524544

W. Kowalczyk, K. Kozłowski, Leader-follower control and collision avoidance for the formation of differentially-driven mobile robots, MMAR 2018 – 23rd International Conference on Methods and Models in Automation and Robotics, 27-30 August 2018, Miedzyzdroje, Poland.

Yoo, S. J., Park, B. S. Connectivity preservation and collision avoidance in networked nonholonomic multi-robot formation systems: Unified error transformation strategy. Automatica, 103, 2019, pp. 274–281, doi:10.1016/j.automatica.2019.02.019